

Preheating Effects on Multiple Material Laser Densification

K. Dai and L. Shaw

Department of Metallurgy and Materials Engineering
Institute of Materials Science
University of Connecticut, Storrs, CT 06269

Abstract: A 3-dimensional thermomechanical model has been developed to study laser powder densification of multiple materials in the multi-materials laser densification (MMLD) process. Thermal and mechanical properties of the materials are porosity- and temperature-dependent. In particular, the effect of the chamber preheating on residual stresses and warping of the part fabricated has been investigated. It is found that the chamber preheating can reduce warping and residual stresses of the laser-processed part. Furthermore, the extent of the preheating effect depends on the laser-scanning pattern. Implications of the simulation result on MMLD have been discussed.

Keywords: Preheating effect, stress, warping, laser densification, finite element modeling

1. INTRODUCTION

The advantages of Solid Freeform Fabrication (SFF) have offered opportunities to develop a cost-effective dental restoration technology, termed as Multi-Materials Laser Densification (MMLD), for permanent fixed prosthodontics which is currently produced by porcelain-fused-to-metal (PFM) restoration process in a majority of dental laboratories [1-2]. In this process, dental restorations are built directly from 3-D computer solid models through two steps. First, dental ceramic and metallic powders are delivered through slurry approaches point-by-point to the desired location. Second, once a layer (or a layer segment) is delivered, the layer is densified using a laser beam scanning in a desired pattern and with adjusted input power density depending on which powder material is under densification. After densification, a new layer of powders will be deposited as described in the first step, which will then be followed again by the second step. This layer-by-layer fabrication process continues until dental restoration is completed. The automation of the MMLD process offers opportunities to present a faster and cheaper dental restoration for dental patients.

The SFF processes investigated by the finite element thermomechanical models include Shape Deposition Manufacturing (SDM) [3-7,10], Laser Engineered Net Shaping (LENS) [8-9], Selective Laser Melting (SLM) [11-12], Direct Metal Laser Beam Sintering (DMLS) [13] and Multi-Material Laser Densification (MMLD) [14-16]. These FE models provide substantial insights into how temperature gradients, thermal transient and residual stresses are developed during SFF processes. It has been shown that SFF processes are accompanied by the development of residual stresses and warping that arise from the thermal gradient in the part due to the local heating via laser beam. Furthermore, the models of MMLD [14-15] have indicated that the mismatch of the thermal and mechanical properties, especially the coefficient of thermal expansion (CTE), between the materials will cause the residual stress and warping when multiple materials are densified in the manufacturing process. Preheating effects on residual stresses and warping have been investigated for the SDM process [7]. However, only single material is

simulated in the SDM process. Furthermore, the starting material considered in the SDM simulation is a solid. Thus, the result from the SDM simulation cannot be applied directly to the MMLD process where multiple powder materials are used as the starting materials [1-2]. In this study a 3-dimensional thermomechanical model has been developed to investigate the preheating effect on residual stresses and distortion of the part made of multiple materials fabricated through the MMLD process. The understanding developed from this study will assist the development of a robust and optimal MMLD process for dental restoration.

2. MODEL DESCRIPTION

As shown in Figure 1, the model investigated consists of a dental porcelain section (porcelain powder shown in white color, porcelain solid shown in dark-gray color) and a dental nickel alloy section (nickel powder shown in dark color, nickel solid shown in gray color). Both porcelain and nickel sections consist of powder initially with a porosity of 33 vol.%. The size of the model is $20 \times 20 \times 1.0 \text{ mm}^3$ and the thickness of each powder layer is 0.5 mm. The part is built layer-by-layer with a laser fabrication sequence that fabricates 3-dimensional bi-material bodies via buildup of the dental alloy section first, followed by buildup of the dental porcelain section, as shown in Figure 1. This has been shown to be an acceptable fabrication sequence in achieving a good control of the dimension and shape of the part made of multiple materials [14]. The porosity of the powder compact is assumed to be temperature-independent before the temperature reaches its melting temperature due to the low thermal conductivity of the powder compact and the local heating by a laser beam with a small beam diameter. As such, the porosity of material in the simulation has been simplified into two levels, one being the initial porosity before laser scanning and the other the zero porosity (i.e., fully dense) after laser scanning. The thermal and mechanical properties of the materials involved and heat losses during fabrication including thermal convection and thermal radiation, however, are temperature- and porosity-dependent. Details of the temperature-dependent material properties can be found in Reference 14, whereas the porosity-dependent properties will be published in a forthcoming paper [17].

Numerical simulation is carried out using the ANSYS commercial finite element package. In order to avoid rotation and translation of the part during simulation, the corner of the first laser-scanned element is constrained. The laser-scanning pattern is shown in Figure 2 where the arrow lines illustrate laser-scanning loci and the circle plotted with a dot line represents the area irradiated by the laser beam. The scanning pattern has its major scanning direction (i.e., the long scanning direction) parallel to the interface of the bi-material. The laser beam heating is modeled as a fixed temperature and moves from a group of surface nodes within the laser beam size of $2 \times 2 \text{ mm}^2$ to the next group of surface nodes as defined by the fabrication sequence, the scanning pattern and the scanning rate. Because each element in this study has a size of 0.67 mm length, 0.67 mm width and 0.5 mm height, there are 3×3 elements are within the range of the beam size, and thus at any given time 16 surface nodes (from 9 surface elements) reach the fixed, user-defined temperature so as to model the heating of laser beam. Such a heating condition mimics the close-loop temperature control used in the MMLD process. The input temperature is set at 1750K when the laser beam scans at the nickel section and 1400K at the porcelain section. The scanning rate is $10 \text{ } \mu\text{m/s}$ and the laser beam moves stepwise by one element each time. Moreover, there is a two-minute cooling time between the fabrication of different layers or sections, which mimics the cooling time during the delivery of one powder layer.

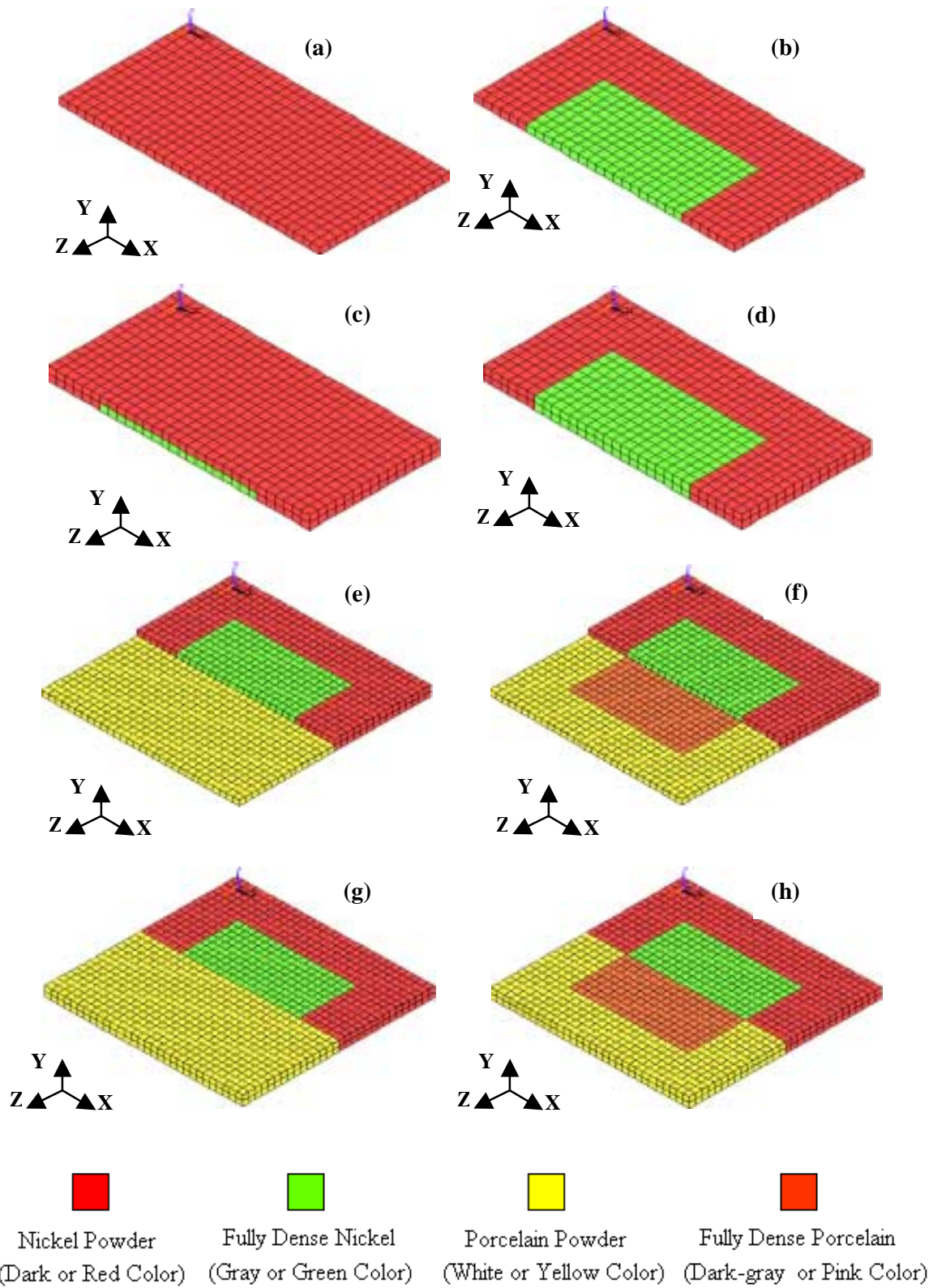


Figure 1. Schematic of the fabrication sequence. The dental alloy section is first fabricated in (a) ~ (d) steps, whereas the porcelain section is fabricated in (e) ~ (h) steps.

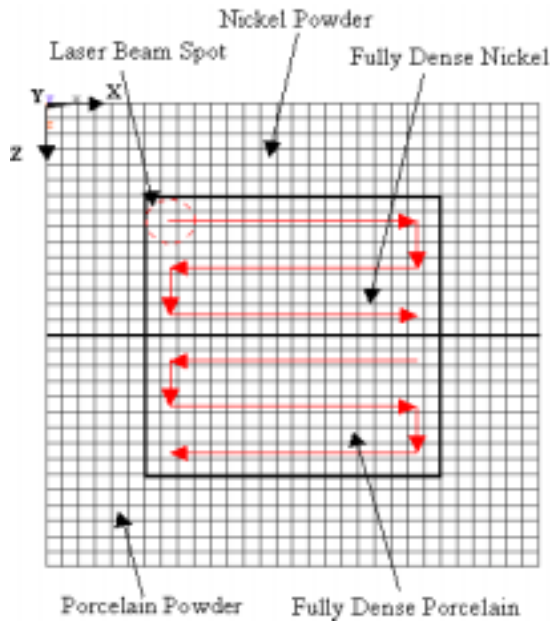


Figure 2. The laser scanning pattern.

In order to evaluate the preheating effect on distortion and stress distribution, preheating of parts being fabricated has been simulated for the following case. The chamber is heated to a desired temperature before laser scanning and kept at that temperature during the entire laser fabrication process. Once the laser beam is turned off, the chamber preheating is stopped and the part being built is allowed to cool down freely. Clearly, such a case is similar to preheating of an entire process chamber uniformly and will effectively reduce the difference between the ambient and laser processing temperatures. In modeling the preheating is achieved by assigning an elevated temperature as the ambient temperature and keeping this temperature throughout the entire process when the laser beam is on. Once the laser beam is turned off, the ambient temperature is set to room temperature to allow the laser-processed part to cool down.

3. SIMULATION RESULTS

Figure 3 shows the residual X- and Z-direction stress distribution and Y-direction warping in the MMLD model forming from porcelain and nickel powders without chamber preheating. The residual X-stresses are predominately controlled by CTE mismatch of the bi-material, which leads to tensile stress in nickel and compressive stress in porcelain near the nickel/porcelain interface. The residual Z-stresses are mainly controlled by the thermal gradient and the warping is concave upward. The development of stresses and warping in the MMLD process has been analyzed in detail [14-16]. Briefly, the residual thermal stress is developed during the cooling process, while the permanent warping is mainly developed during the heating process and is predominately controlled by transient thermal stresses rather than residual thermal stresses [16]. Detailed examination of the temperature field and transient stress distribution during laser scanning indicates that the fundamental reason for the out-of-plane warping is the presence of temperature differences between the top and bottom surfaces of the plate. This temperature difference in turn generates transient stresses that are different between the top and bottom surfaces, thereby leading to the asymmetric deformation between the top and bottom surfaces and thus the out-of-plane warping [16]. Since the state and magnitude of transient

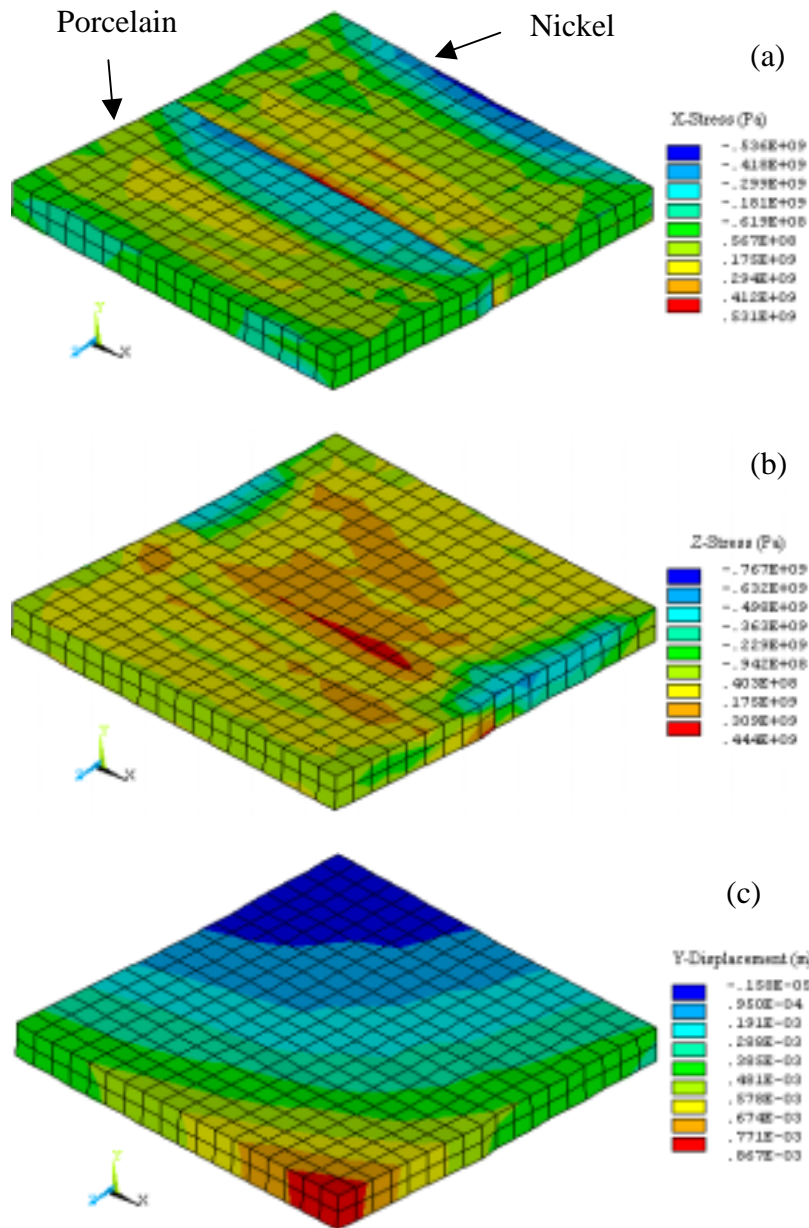


Figure 3. The residual (a) x- and (b) z-direction stress, and (c) the residual y-direction displacement distribution.

thermal stresses are the major factors in determining distortion, it is expected that any method that can reduce temperature gradients in parts being fabricated can minimize distortion. Chamber preheating and substrate preheating are such methods.

In the present study, the models with chamber preheating at a temperature of 400K, 500K, 600K, 700K and 800K are simulated. The simulation results indicate that the distribution patterns of residual stresses and out-of-plane warping are similar with the model without preheating (Figure 3). However, the distribution patterns of transient stresses are different. In the model without preheating, the nickel section is subjected to tensile stresses near the interface when laser is scanning the porcelain section at the region away from the interface. In contrast, this distribution pattern is changed to partly tensile and compressive stresses or even fully compressive stresses with the increase in the preheating temperature. This is due to less thermal shrinkage of the nickel section when the chamber preheating is applied.

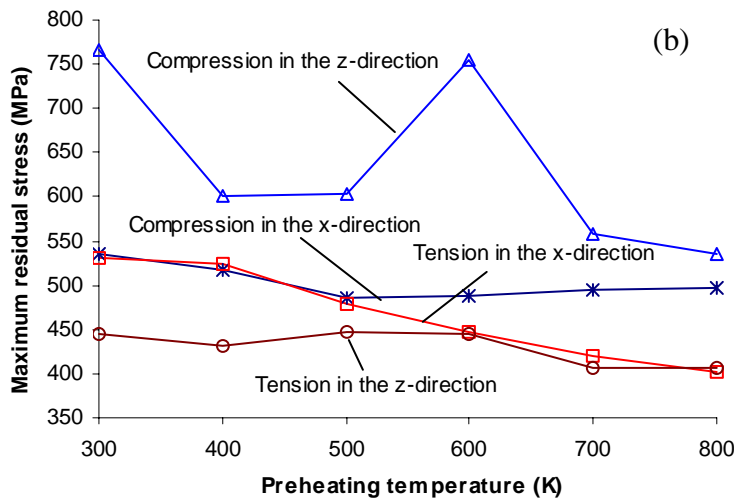
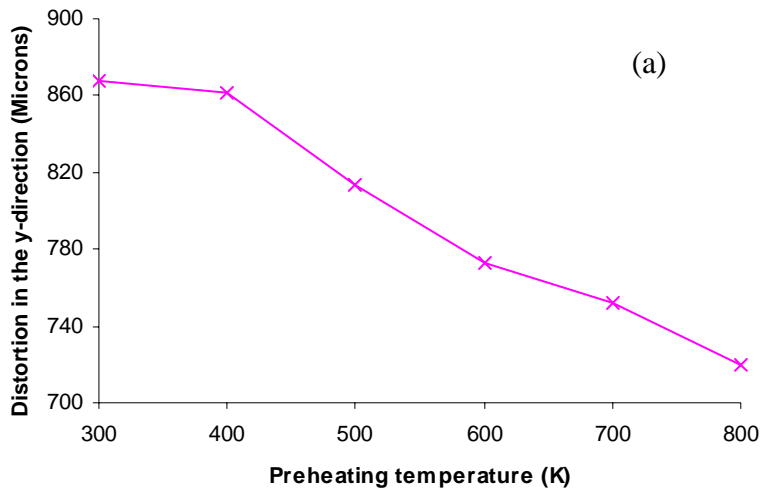


Figure 4. (a) Distortion in the y-direction and (b) residual stresses versus the chamber preheating temperature in the bi-material model (nickel and porcelain).

Shown in Figure 4 are the out-of-plane distortion and the maximum values of residual stresses in the X- and Z-direction as a function of the chamber preheating temperature in the bi-material model. It can be seen that the out-of-plane warping decreases monotonically with the increase in the preheating temperature. The warping decreases by about $30\mu\text{m}$ for every 100K increase in the preheating temperature. Compared with the model without preheating, the warping of the model with preheating at 800K decreases by about 17%. It is also found from Figure 4(b) that residual stresses also decrease when raising the preheating temperature except for the residual Z-stresses with a preheating temperature of 600K. With a chamber preheating of 800K the residual tensile X-stress and compressive Z-stress decrease by 25% and 30% in comparison with that obtained without preheating, respectively. At the same time the preheating of 800K also leads to a reduction of the residual compressive X-stress and tensile Z-stress (about 9%). It is clearly that the chamber preheating results in a smaller thermal gradient before cooling, which in turn leads to more uniform cooling and thus smaller residual stresses. The present

simulation suggests that high quality parts fabricated via the MMLD process should be obtained with a chamber preheating temperature larger than 700K.

Effects of the chamber preheating on residual stresses and warping in single solid material (e.g., nickel) have also been evaluated. Shown in Figure 5 are the two laser scanning patterns, pattern I and II, evaluated. The model has a single layer of nickel plate with a dimension of $60 \times 60 \times 2.0 \text{ mm}^3$ and a chamber preheating of 800K is applied. A comparison between the models with and without preheating indicates that the out-of-plane warping in the scanning pattern I and II decreases by 32% and 73% respectively with the application of the preheating at 800K. Furthermore, residual stresses are also reduced, although small (less than 11%), by preheating for both scanning patterns.

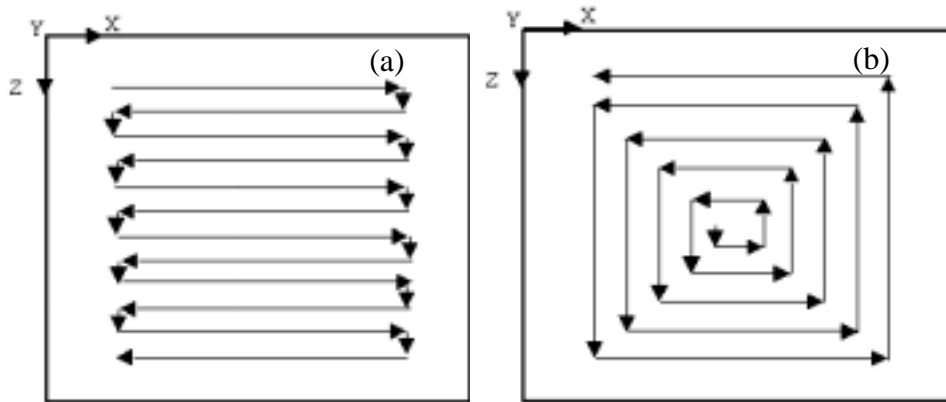


Figure 5. Schematic of laser scanning pattern (a) I and (b) II for nickel plate [16]

4. CONCLUSIONS

The present finite element modeling has shown that the chamber preheating could result in less out-of-plane warping and residual stresses in parts made of multiple materials fabricated using a moving laser beam. The preheating effect also depends on the laser-scanning pattern. The laser scanning pattern II, which changes the scanning direction constantly, provides larger reductions in the out-of-plane warping and residual thermal stresses than the pattern I. The maximum reduction in warping and residual stresses can be achieved by coupling of chamber preheating and scanning pattern II. The underlying mechanism responsible for the effect of chamber preheating is the reduction of temperature gradients between the top and bottom surfaces of the part being fabricated, which in turn gives rise to smaller transient stresses, thereby a smaller difference in the asymmetric deformation between the top and bottom surfaces of the part and thus smaller out-of-plane warping.

Acknowledgements – The authors gratefully acknowledge financial support provided by the National Science Foundation under Grant No: DMI-9908249.

REFERENCES

1. X.X. Li, J.W. Wang, A. Augustine, L.L. Shaw, H. L. Marcus, T. B. Cameron, “Microstructure Evaluation for Laser Densification of Dental Porcelains”, in Proc. 12th SFF Symp., edited by D. L. Bourell, et al., The University of Texas, 2001, pp. 195-202.

2. J.W. Wang, X.X. Li, L. L. Shaw, H. L. Marcus, T.B. Cameron, "Powder Delivery in Dental Restoration Rapid Prototyping Process", in Proc. 12th SFF Symp., edited by D. L. Bourell, et al., The University of Texas, 2001, pp. 546-552.
3. Chin, R.K., Beuth, J.L. and Amon, C.H., "Thermomechanical Modeling of Molten Metal Droplet Solidification Applied to Layered Manufacturing," *Mech. Mater.*, Vol. 24, 1996, pp. 257-271.
4. Amon, C.H., Beuth, J.L., Merz, R., Prinz, F.B. and Weiss, L.E., "Shape Deposition Manufacturing with Microcasting: Processing, Thermal and Mechanical Issues," *J. Manufact. Sci. Eng.*, Vol. 120, No. 3, 1998, pp. 656-665.
5. Chin, R.K., Beuth, J.L. and Amon, C.H., "Successive Deposition of Metals in Solid Freeform Fabrication Processes Part 1: Thermomechanical Models of Layers and Droplet Columns," *Journal of Manufacturing Science and Engineering*, Vol. 123, No. 4, 2001, pp. 623-631.
6. Chin, R.K., Beuth, J.L. and Amon, C.H., "Successive Deposition of Metals in Solid Freeform Fabrication Processes Part 2: Thermomechanical Models of Adjacent Droplets," *Journal of Manufacturing Science and Engineering*, Vol. 123, No. 4, 2001, pp. 632-638.
7. Ong, R., Beuth, J.L. and Weiss, L.E., "Residual Stress Control Issues for Thermal Deposition of Polymers in SFF Processes," in Proc. 11th SFF Symp., edited by D. L. Bourell, et al., The University of Texas, 2000, pp. 209-218.
8. Vasinonta, A., Beuth, J.L. and Griffith, M.L., "A Process Map for Consistent Build Conditions in the Solid Freeform Fabrication of Thin-Walled Structures," *Journal of Manufacturing Science and Engineering*, Vol. 123, No. 4, 2001, pp. 615-622.
9. Vasinonta, A., Beuth, J.L., and Ong, R., "Melt Pool Size Control in Thin-Walled and Bulky Parts via Process Maps," in Proc. 12th SFF Symp., edited by D. L. Bourell, et al., The University of Texas, 2001, pp. 432-440.
10. A. H Nickel, DM Barnett, FB Prinz, "Thermal Stresses and Deposition Patterns in Layered Manufacturing", *Materials Science and Engineering*, A317 (2001) pp. 59-64.
11. M. Shiomi, M. Matsumoto, K. Osakada, F. Abe, "Two-Dimensional Finite Element Simulation of Laser Rapid Prototyping, Simulation of Materials Processing: Theory, Methods and Applications", Balkema (K. Mori ed.), Proc. NUMIFORM 2001, (2001), pp. 1059-1064
12. M. Matsumoto, M. Shiomi, K. Osakada and F. Abe, "Finite Element Analysis of Single Layer Forming on Metallic Powder Bed in Rapid Prototyping by Selective Laser Processing", *Int. J. Machine Tools & Manufacture*, 42 (2002), pp. 61-67.
13. F. Niebling, A. Otto, "FE-Simulation of the Selective Laser Sintering Process of Metallic Powders", *Proceedings of 3rd International Conference on Laser Assisted Net Shaping (LANE2001)*, pp. 371-382.
14. K. Dai and L. Shaw, "Thermal and Stress Modeling of Multi-Material Laser Processing", *Acta Mater.*, 49 (2001) 4171-4181.
15. K. Dai and L. Shaw, "The Size Effect on Stresses and Distortion of Laser Processed Multi-Material Components", submitted to *Metall. Mater. Trans.* (2002).
16. K. Dai and L. Shaw, "Distortion Minimization of Laser-Processed Components through Control of Laser Scanning Patterns", accepted by *Rapid Prototyping Journal*. (2002).
17. K. Dai and L. Shaw, "Thermal and Mechanical Finite Element Modeling of Laser Forming from Metal and Ceramic Powders", unpublished research (2002).